Biophysics of amplitude-modulated giga-hertz electromagnetic waves stimulation

Fatima Ahsan*, Aravind C. Govindaraju[†‡], Robert M. Raphael[‡], Taiyun Chi*, Sameer A. Sheth[§], Wayne Goodman[¶], and Behnaam Aazhang*

*Department of Electrical and Computer Engineering, Rice University, Houston, TX, USA.

[†]Applied Physics Graduate Program, Smalley-Curly Institute, Rice University, Houston, TX.

[‡]Department of Bioengineering, Rice University, Houston, TX, USA.

[§]Department of Neurosurgery, Baylor College of Medicine, Houston, TX, USA.

[¶]Menninger Department of Psychiatry and Behavioral Sciences, Baylor College of Medicine, Houston, TX, USA.

Email: fatima.ahsan@rice.edu, ag105@rice.edu, rraphael@rice.edu, taiyun.chi@rice.edu, sameer.sheth@bcm.edu, wayne.goodman@bcm.edu, aaz@rice.edu

2023 57th Asilomar Conference on Signals, Systems, and Computers | 979-8-3503-2574-4/23/$31.00 ©2023 IEEE | DOI: 10.1109/IEEECONF59524.2023.10476737

***Abstract*—This paper presents the biophysical modeling for neuronal stimulation caused by amplitude-modulated giga-hertz (GHz) electromagnetic (EM) waves. We model a 1D cable equation for electrical signal propagation in a vestibular ganglion neuronal fiber and use Hodgkin-Huxley formalism to model voltage-dependent channel conductances. We find out that for a given stimulation signal strength, the GHz waveform amplitude-modulated at a low frequency of Δf causes neuronal firing with the frequency of Δf whereas the continuous wave GHz did not elicit any neuronal firing. Moreover, the voltage-dependent channel gating dynamics of the Δf amplitude-modulated GHz stimulation matches that of a simple low frequency stimulation at Δf. Additionally, we find that the modulation depth controls the firing rate of the neurons. The significance of this property is that the amplitude modulation caused by the interference of two similar high frequency signals could be leveraged to focally excite neurons at depth without stimulating overlying cortical regions. These theoretical predictions based on the Hodgkin-Huxley model can later be tested experimentally.**

I. Introduction

Nearly 30% of the global burden of diseases is attributed to brain disorders, such as Parkinson's disease, epilepsy, and depression. After drug interventions to treat these disorders fail, Deep Brain Stimulation (DBS) is the most commonly used solution. DBS is a neuro-surgical procedure in which electrodes are implanted in the brain. However, its potential is limited by its surgical complications, like brain infection or vessel ruptures leading to stroke [1]. Non-invasive advances in DBS, like Transcranial Electrical Stimulation (TES) and Transcranial Magnetic Stimulation (TMS), are promising but have limitations [2], [3]. First, they are bulky and non-portable. For comparison, targeted TES is applied through 64 or more electrodes worn as a head cap [4], and TMS is applied through bulky coils placed near the head [5], making them difficult to use for diseases that require continuous stimulation, such as Parkinson's disease. Second, the strength of electric field intensity deep inside the brain is weak and achieved at the expense of strongly stimulating overlying cortical regions, reducing their effectiveness [6], [7].

We thank The Robert and Janice McNair Foundation for supporting this work.

To overcome these challenges, recently the idea of amplitude-modulation caused by the the temporal interference of two giga-hertz (GHz) Electromagnetic (EM) waves, at similar frequencies of f_1 and $f_1 + \Delta f$, to stimulate the neurons, was proposed [8]. This methodology is termed as **EMvelop stimulation** and is illustrated in Fig. 1. The key motivation in EMvelop stimulation for using two similar high frequency signals to elicit neuronal firing is that the signal at f_1 (shown in black in Fig. 1) and the signal at $f_1 + \Delta f$ (shown in blue in Fig. 1) are both high frequency signals and are not followed by the neurons due to the low-pass filtering property of the neural membrane [9]. However, deep in the brain tissue where both of these signals overlap, they create a high frequency signal (shown in green in Fig. 1) that has its amplitude-modulated at Δf (shown in the dashed-green in Fig. 1). This resultant low frequency amplitude-modulation of the high frequency interfering signal is hypothesized to modulate the activity of the neurons deep inside the brain tissue where the the interference happens, sparing the overlying cortical regions that only experience the high frequency signal. This approach is inspired by the prior work of using two similar kilohertz currents for transcranial electrical stimulation [10]. However, instead of using kilohertz currents, [8] proposed using giga-hertz (GHz) electromagnetic (EM) waves generated by endocranial antenna arrays to increase the stimulation intensity and target stimulation precisely inside the brain tissue, while minimizing the form factor of the stimulation device.

Prior work on EMvelop stimulation has only focused on the spatial distribution of amplitude-modulated electric fields induced by antenna arrays placed endocranially on the human brain tissue [8]. Additionally, although several experimental works report amplitude-modulated EM waves influencing neuronal activity or behaviour with a much lower field strength than a continuous wave EM wave [11]–[13], these studies did not propose biophysical models to understand the neuronal response. Moreover, we are not aware of any biophysical modeling studies that investigate how such a stimulation protocol compares to a simple low-frequency stimulation protocol. Some works have modeled the interaction of EM waves with neurons [14], [15], however, their modeling is only limited to the calculation of the voltage induced across the neuronal fiber as a result of continuous wave EM wave stimulation.

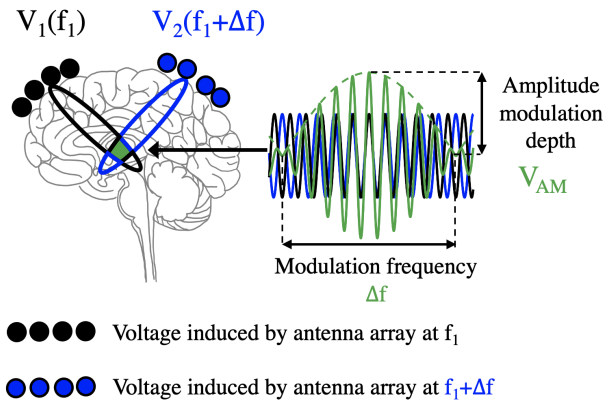

Fig. 1: EMvelop stimulation methodology. Superposition of the voltage induced due to GHz electric fields from two antenna arrays, shown in black and blue, differing by a small frequency offset Δf creates the EMvelop signal, shown in green, whose amplitude is modulated at Δf. V_1 and V_2 are voltages induced by each array, defined in (2), and V_{AM} is the peak-to-peak value of the dashed envelope, defined in (3).

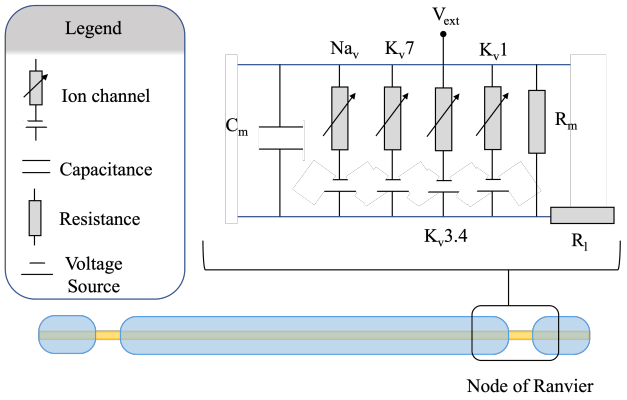

Fig. 2: Illustration of the myelinated neuronal fiber with nodes of Ranvier. An external voltage V_{ext} is simultaneously being applied at all points of the fiber.

The contribution of this work to present the first biophysical modeling investigation on the effect of amplitude-modulated GHz stimulation on the neurons. We make the following contributions:

- We use 1D cable equation and Hodgkin-Huxley formulation computational modeling to understand the interaction of EM waves with individual neuronal fibers.
- We find that neurons respond to an amplitude-modulated EM wave stimulation and not to the continuous wave EM stimulation of the same intensity. Moreover, the amplitude-modulation depth controls the firing rate of the neurons.
- Additionally, we find that the channel dynamics of an amplitude-modulated GHz EM wave stimulation matches that of a direct low frequency stimulation.

The paper is organized as follows. Section II describes the candidate stimulation waveforms, the cable theory, and the Hodgkin-Huxley formalism. Section III evaluates the voltage across the neuronal fiber due to these stimulation waveforms and compares their voltage dependent channel gating dynamics. Section IV discusses our future work and Section V discusses our results and concludes the work.

II. Methods

To investigate the general principles governing the interaction of EM waves with neurons, we used a single myelinated neuronal fiber with nodes of Ranvier for signal exchange. This setup shown in Fig. 2. A 1D model of a section of vestibular ganglion nerve fiber was adapted from [16]. The relevant kinetics of voltage-gated sodium and potassium ion-channels are reproduced below. The response of this fiber to external stimulation was then studied. The external voltage V_{ext} is applied to all the points of the fiber simultaneously, and the resultant change in the potential across the 1D neuronal fiber is calculated. Cable and Hodgkin-Huxley equations implemented calculate the voltage and currents moving across the fiber.

A. Stimulation waveforms

We studied the effect of three stimulation waveforms V_{ext} detailed below:

EMvelop stimulation: Suppose $V_1(t)$ and $V_2(t)$ are the two interfering waveforms with frequencies f_1 and $f_2 = f_1 + \Delta f$, respectively, where $\Delta f \ll f_1$. $V_1(t)$ and $V_2(t)$ are the voltage induced across the neuronal fiber as a result of EM wave stimulation, which can be calculated by methods highlighted in [14], [15]. Therefore, the applied stimulation is

$$V_{ext}(t) = V_1(t) + V_2(t), \tag{1}$$
$$V_{ext}(t) = A_1 sin(2\pi f_1 t) + A_2 sin(2\pi f_2 t). \tag{2}$$

The amplitude-modulation depth V_{AM} is given by

$$V_{AM} = 2 \cdot min(|A_1|, |A_2|). \tag{3}$$

Low frequency stimulation: In this case, we excite the neuronal fiber with an external voltage at the difference frequency of Δf. Therefore, the applied stimulation is

$$V_{ext}(t) = A_1 sin(2\pi \Delta f t). \tag{4}$$

High frequency stimulation: In this case, we excite the neuronal fiber with the high frequency of f_1. Therefore, the applied stimulation is

$$V_{ext}(t) = A_1 sin(2\pi f_1 t). \tag{5}$$

B. Cable Theory

Neuronal cable theory calculates the voltage and currents moving across the neuronal fiber due to external stimulation [17]. The circuit representation of a segment of the fiber is shown in the Fig. 2. The total length of the fiber is $416\mu m$ and consists of (left to right) $71\mu m$ myelinated, $2\mu m$ unmeylinated, $300\mu m$ myelinated, $2\mu m$ unmeylinated, and $41\mu m$ of myelinated segments. The voltage across the fiber V_f is defined as $V_f = \phi - V_{ext}$, where ϕ is the voltage across the fiber without any external stimulation and V_{ext} is the applied external voltage, defined in section II-A. V_f is calculated by solving the cable equation

$$\frac{1}{R_l}\frac{d^2V_f}{dx^2} = C_m\frac{dV_f}{dt} + \frac{V_f}{R_m}. \tag{6}$$

Here, R_m is the membrane resistance, C_m is the membrane capacitance, and R_l is the longitudinal resistance. Additionally, $R_l = \rho_l \frac{l}{A}$, where l, A, ρ_l are the length, area, and longitudinal resistivity of the fiber, respectively. We re-arrange (6) to get

$$2\rho_l C_{m,s} \frac{dV_f}{dt} - r_f \frac{d^2 V_f}{dx^2} = -2\rho_l J_m. \tag{7}$$

Here, r_f is the radius of the fiber, $I_m = V_f/R_m = 2\pi r_f J_m l$ and $C_m = 2\pi r_f C_{m,s}$. Here, $C_{m,s}$ is the specific membrane capacitance and J_m is the membrane current density. This re-arrangement expresses the cable equations in terms of specific capacitative and resistive membrane currents as well as the longitudinal current in the fiber.

C. Hodgkin-Huxley Modeling

At the nodes of Ranvier, the model consisted of the sodium current (J_{Na_v}), K_v7 potassium current (J_{K_v7}), $K_v3.4$ potassium current ($J_{K_v3.4}$), and K_v1 potassium current (J_{K_v1}) [16]. The net current passing through the membrane J_m is given due to each of the ionic currents $x \in \{Na_v, K_v7, K_v3.4, K_v1\}$

$$J_m = \sum_x J_x = J_{Na_v} + J_{K_v7} + J_{K_v3.4} + J_{K_v1}. \tag{8}$$

To model the ionic currents passing through the membrane, we use the Hodgkin-Huxley formalism [18]

$$J_x = g_x \cdot (V_f - V_{x,eq}), \tag{9}$$

where g_x is the conductance of the ion and $V_{x,eq}$ is its equilibrium potential. The conductance for each of the currents can be written in terms of their gating variables as

$$g_{Na_v} = \overline{g}_{Na_v} m^3 h, \tag{10}$$

$$g_{K_v7} = \overline{g}_{K_v7} n_{K_v7}, \tag{11}$$

$$g_{K_v3.4} = \overline{g}_{K_v3.4} n_{K_v3.4} s_{K_v3.4}, \tag{12}$$

$$g_{K_v1} = \overline{g}_{K_v1} n_{K_v1}. \tag{13}$$

Here, m and h represent the channel activation and inactivation variables for sodium, respectively. Additionally, $n_{K_v7}, n_{K_v3.4}$ and n_{K_v1} are the activation variables for K_v7, $K_v3.4$, and K_v1 potassium channels, respectively, and $s_{K_v3.4}$ is the inactivation variable for of the $K_v3.4$ potassium channel. Moreover, $\overline{g}_{Na_v}, \overline{g}_{K_v7}, \overline{g}_{K_v3.4}$, and $\overline{g}_{K_v1}$ is the maximum conductance of the sodium channel, K_v7 potassium channel, $K_v3.4$ potassium channel, and K_v1 potassium channel, respectively. The $V_{x,eq}$ and the maximum conductance for each of the currents is given in Table I.

Current	Equilibrium Potential	Maximum Conductance
J_x	$V_{x,eq}[mV]$	$\overline{g}_x[nS/\mu m^2]$
Na_v	63.8	120
K_v7	-88.4	0.1
$K_v3.4$	-88.4	0.2
K_v1	-88.4	0.13

TABLE I: Values of equilibrium potential and maximum conductance used in our model.

The time constants and steady-state activation for each of the gating variables $X \in \{m, h, n_{K_v7}, n_{K_v3.4}, n_{K_v1}, s_{K_v3.4}\}$ is given by solving

$$\tau_X(V_f) \frac{d(X)}{dt} = X_\infty(V_f) - X. \tag{14}$$

The table II summarizes time constant (τ_X) and steady-state activation (X_∞) for each of the gating variable X.

III. Results

We implement the cable and Hodgkin-Huxley equations in COMSOL Multiphysics v6.0 [19] to calculate the voltage and currents moving across the fiber in the time-domain. We use frequencies $f_1 = 1$ GHz and $\Delta f = 100$ Hz in (2). In the simulated geometry of the fiber, described in Section II-B, $r_f = 1.5\mu m$, $C_{m,s} = 0.01 pF/\mu m^2$, and $\rho_l = 1 M\Omega \mu m$.

Fig. 3A shows the result of stimulation of the neuronal fiber with stimulation signal of 100 Hz. We see that the neurons fire an action potential with almost every cycle of the 100 Hz stimulation waveform. Next, shown in Fig. 3B, we excite the neuronal fiber with the EMvelop signal, i. e., 1 GHz amplitude-modulated with 100 Hz. The neurons fire an action potential with every cycle of the EMvelop signal. Finally, the result of exciting the neuronal fiber with 1 GHz waveform is shown in Fig. 3C. We can see that the continuous wave GHz stimulation fails to excite the neurons, as we hypothesized. The voltage across the neuron stays at the resting membrane potential, and action potentials do not occur. This shows that amplitude modulation of the GHz waveform is necessary to cause an action potential.

Next we calculated the net membrane current density J_m as a result of the external stimulation. Fig. 4A shows the result of stimulation of neuronal fiber with stimulation signal of 100 Hz. We can see that the current flows across the neuronal membrane with almost every cycle of the 100 Hz stimulation. Fig. 4B shows the result of exciting the neurons with 1 GHz waveform amplitude-modulated with 100 Hz. The current flows through the neuronal membrane with every cycle of the EMvelop signal. Fig. 4C shows the result of exciting the neuronal fiber with 1 GHz waveform. We see negligible current flowing through the membrane as a result of continuous wave GHz stimulation. This once again reinforces that amplitude-modulation of the GHz waveform is necessary to cause a current to flow through the neuronal membrane.

We also evaluated the open probabilities for gating variables X for both 100 Hz and EMvelop stimulation. This is shown in Fig. 5. For both kinds of stimulations, we observe identical patterns. An action potential occurs when both m and h are high. However, as the membrane potential increases, h goes to zero, which shuts off the spike. Additionally, note that n_{K_v7} keeps rising because the time constant of the channel is too slow for the probability to fall before the rise in probability towards $n_{K_v7,\infty}$ during the subsequent action potential.

Fig. 6A shows the channel gating steady-state values as a result of 100 Hz stimulation and Fig. 6B for EMvelop stimulation. It shows the steady state values for different gating variables over the course of the sinusoidal variation in V_{ext}. The spread in the curves occurs because the changes in V_f vary slightly between cycles as the internal potential of the fiber (ϕ) is different each time. Additionally, the time constants for the channel gating variables as a result of 100 Hz and EMvelop stimulation waveform are shown in Fig. 7A and B, respectively, and are comparable.

Previous works hypothesized that the neuronal firing is also governed by the modulation depth [8], [10], defined in (3).

X	$\tau_X(V_f)$	$X_\infty(V_f)$
m	$(1+exp(-\frac{V_f+41.58}{5.733}))^{-1}\cdot(1+exp(-\frac{V_f+8.295}{16.28}))^{-1}+0.2$	$(1+exp(-\frac{V_f+40}{8}))^{-1}$
h	$0.0001452exp(-0.2211V_f)+0.2382$	$(1+exp(-\frac{V_f+69}{7.6}))^{-1}$
$n_{K_v}7$	$1.2\cdot exp(-0.08V_f)(1+exp(-\frac{V_f+47}{8}))^{-1}$	$(1+exp(-\frac{V_f+47}{8}))^{-1}$
$n_{K_v}3.4$	$7.05\cdot exp(-0.05589V_f)\cdot(1+exp(-\frac{V_f+31.3}{8.5}))^{-1}$	$(1+exp(-\frac{V_f+31.3}{8.5}))^{-1}$
$n_{K_v}1$	$3.7ms$	$(1+exp(-\frac{V_f+44}{7.1}))^{-1}$
$s_{K_v}3.4$	$25.4ms$	$(1+exp(-\frac{V_f+65.84}{5.51}))^{-1}$

TABLE II: The time constant (τ_X) and steady-state activation (X_∞) for a gating variable X.

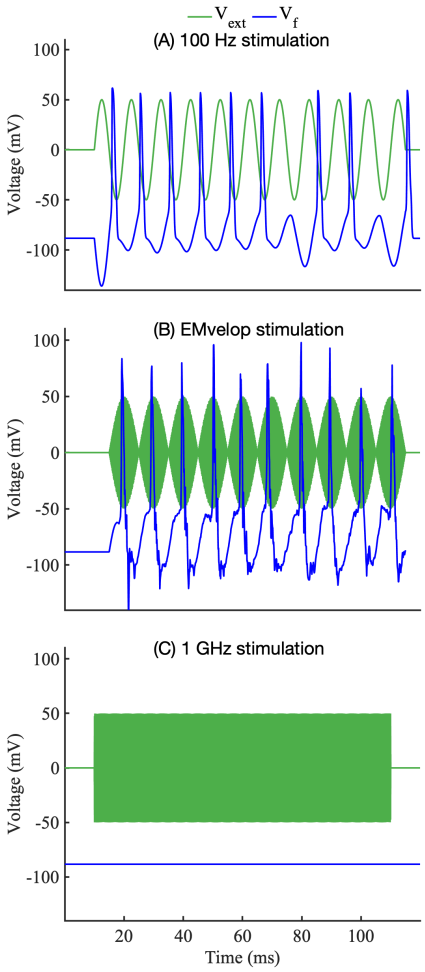

Fig. 3: The input voltage signal V_{ext} to the fiber is shown in green, and the voltage across the neuronal neurons V_f is shown in blue. *Panel A*. The result of stimulation of neuronal fiber with sinusoidal voltage of 100 Hz. Neuronal firing is entrained to to the stimulation frequency of 100 Hz. *Panel B*. The result of exciting the neurons with EMvelop signal, i.e., GHz waveform amplitude-modulated with 100 Hz. The neurons fire an action potential with every cycle of the EMvelop signal. *Panel C*. The result of exciting the neuronal fiber with 1 GHz waveform. We see that the continuous wave GHz stimulation fails to excite the neurons, as hypothesized.

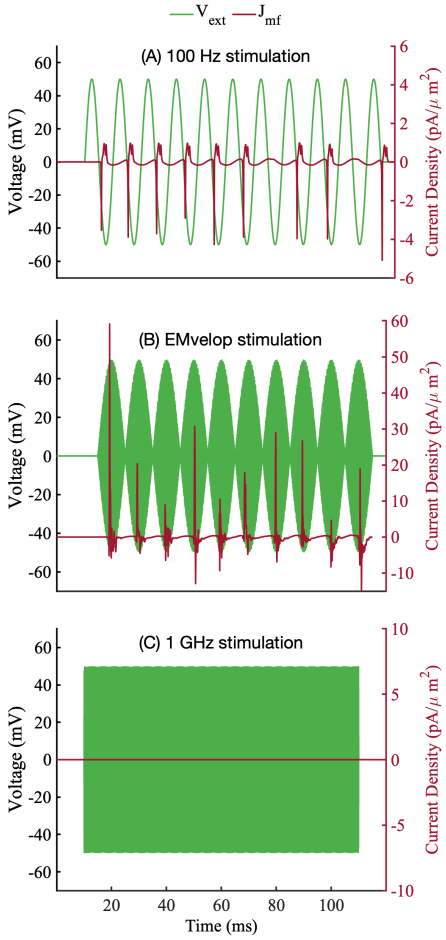

Fig. 4: The input voltage signal to the fiber is shown in green, and the net membrane current density J_m flowing through the neuronal membrane is shown in brown. *Panel A*. The result of stimulation of neuronal fiber with stimulation signal of 100 Hz. Current flows across the neuronal membrane with almost every cycle of the 100 Hz stimulation waveform. *Panel B*. The result of exciting the neurons with EMvelop signal, i.e., GHz waveform amplitude-modulated with 100 Hz. Once again we see that the current flows through the neuronal membrane with every cycle of the EMvelop signal. *Panel C*. We see that the continuous wave 1 GHz stimulation does not cause sufficient current to flow through the membrane, as hypothesized.

Hence, next, we evaluated the effect of change of amplitude-modulation depth while keeping the maximum peak of the sinusoidal amplitude the same (i.e., $50mV$). We tested for the following three different cases in 2): i) $A_1 = 1mV, A_2 = 49mV$, ii) $A_1 = 5mV, A_2 = 45mV$, and iii) $A_1 = 15mV, A_2 = 35mV$. As shown in Fig. 8, even a relatively small amount of amplitude-modulation seems to influence neuronal excitation. However, maximum neuronal stimulation occurs at maximum

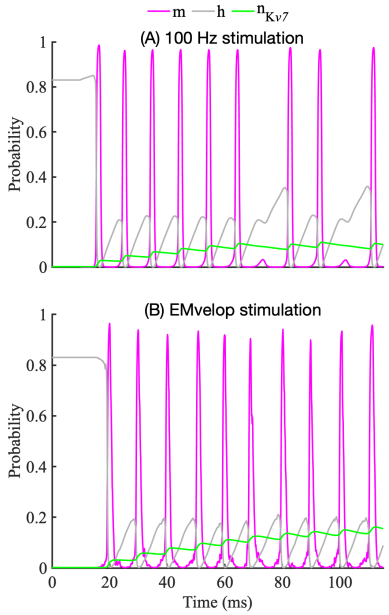

Fig. 5: Plots of m, h, n_{K_v7} as a result of (Panel A) 100 Hz and (Panel B) EMvelop stimulation waveform. The voltage dependent gating dynamics of both stimulation strategies are comparable.

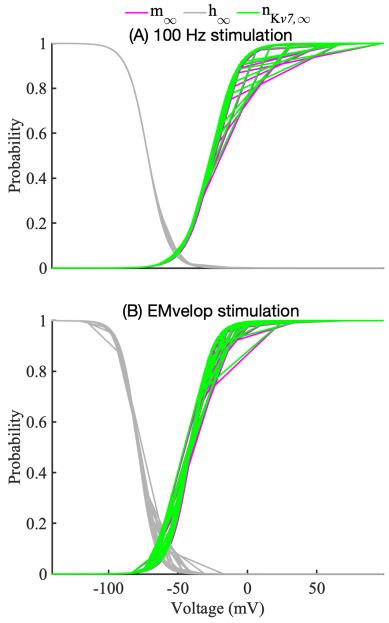

Fig. 6: The channel steady-state probabilities for $m_\infty, h_\infty, n_{K_v7,\infty}$ as a result of (Panel A) 100 Hz and (Panel B) EMvelop stimulation waveform. The voltage dependent channel steady-state probabilities of both stimulation strategies are comparable.

amplitude-modulation depth. These model predictions support earlier published results that amplitude-modulation depth of the interfering sinusoidal waves is the driving force for amplitude-modulated high-frequency stimulation waveforms [20, 1].

IV. Future Work

Our modeling supports the hypothesis of EMvelop stimulation, that we can selectively stimulate deep brain targets which experience the supposition of the two interfering waveforms, whereas superficial regions that only experience the high

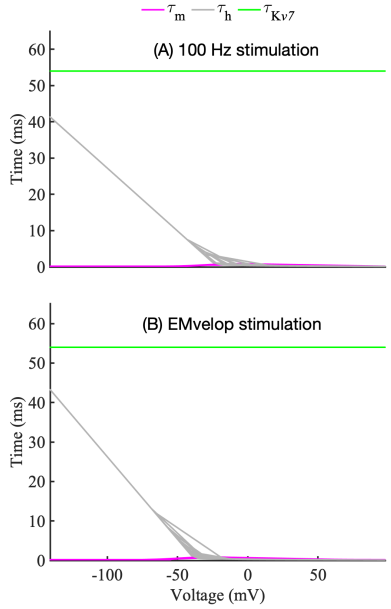

Fig. 7: The time constants for the gating variables for $\tau_m, \tau_h, \tau_{n_{K_v7}}$ as a result of (Panel A) 100 Hz and (Panel B) EMvelop stimulation waveform. The voltage dependent time constants of both stimulation strategies are comparable.

frequency stimulation do not experience neuronal stimulation. Such a theoretical study is an essential step in informing animal experiments, as this determines the stimulation intensity V_{ext} needed to excite the neurons, the effect of carrier frequency f_1, and the difference frequency Δf on the firing rate of the neurons. In our future work, we aim to further refine our understanding of the effects of different parameter values on these driving mechanisms of the EMvelop stimulation. Additionally, we plan to study the effect of EMvelop stimulation other types of neurons as well, such as those found in the hippocampus and the cortex. In future, we will also test these predictions for the EM waves interaction with biological tissues to cause neuronal stimulation experimentally.

V. Discussion and Conclusions

In this paper, we presented a computational modeling framework for evaluating the effect of low-frequency amplitude-modulated GHz EM waves on neurons. We used cable theory and Hodgkin-Huxley formalism to evaluate the voltage and current moving across the neuronal fiber. We found that amplitude-modulation of the high frequency GHz waves entrains the neural activity. In comparison, continuous wave EM wave of same intensity does not cause the neurons to fire. Additionally, we found that the neuronal firing patterns as well as the currents and voltage-gated channel dynamics of the amplitude-modulated GHz stimulation obeyed similar characteristics as that of a low frequency stimulation at the modulation beat frequency. The significance of our proof-of-principle work is that it emphasizes the feasibility of utilizing the amplitude-modulation caused due to temporal interference of two similar GHz waves deep inside the brain tissue. This promises to be a much more focused way of stimulating the brain targets than state-of-the-art techniques. This also opens the possibility to deliver focal therapeutic stimulation stimulation in a portable fashion with EM waves generated with small endocranially implantable antenna arrays.

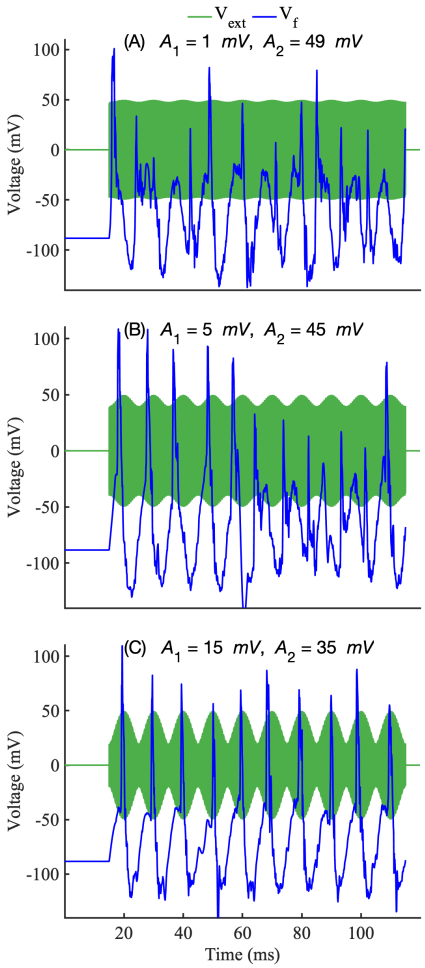

Fig. 8: The input voltage signal to the fiber is shown in green, and the response of neurons is shown in blue. The amplitude-modulation depth is successively increased (top panel to bottom panel). We can see that minimal firing occurred at small amplitude-modulation modulation depth (Panel A) and the most consistent neuronal firing occurred at the maximum amplitude-modulation modulation depth (Panel C), indicating that the amplitude-modulation depth controls the firing rate.

REFERENCES

[1] A. R. Zamora *et al.*, "Evolving Applications, Technological Challenges and Future Opportunities in Neuromodulation: Proceedings of the Fifth Annual Deep Brain Stimulation Think Tank," *Frontiers in Neuroscience*, vol. 11, pp. 734–760, 2018.

[2] E. Dayan, N. Censor, E. R. Buch, M. Sandrini, and L. G. Cohen, "Noninvasive brain stimulation: from physiology to network dynamics and back," *Nature Neuroscience*, vol. 16, pp. 838–844, 2013.

[3] P. M. Rossini *et al.*, "Non-invasive electrical and magnetic stimulation of the brain, spinal cord, roots and peripheral nerves: Basic principles and procedures for routine clinical and research application. An updated report from an I.F.C.N. Committee," *Clinical Neurophysiology*, vol. 126, pp. 1071–1107, 2015.

[4] J. P. Dmochowski, A. Datta, M. Bikson, Y. Su, and L. C. Parra, "Optimized multi-electrode stimulation increases focality and intensity at target," *Journal of Neural Engineering*, vol. 8, p. 046011, 2011.

[5] L. J. Gomez, S. M. Goetz, and A. V. Peterchev, "Design of transcranial magnetic stimulation coils with optimal trade-off between depth, focality, and energy," *Journal of Neural Engineering*, vol. 15, p. 046033, 2018.

[6] Z.-D. Deng, S. H. Lisanby, and A. V. Peterchev, "Electric field depth–focality tradeoff in transcranial magnetic stimulation: simulation comparison of 50 coil designs," *Brain stimulation*, vol. 6, no. 1, pp. 1–13, 2013.

[7] Y. Huang and L. C. Parra, "Can transcranial electric stimulation with multiple electrodes reach deep targets?" *Brain Stimulation*, vol. 12, 2019.

[8] F. Ahsan, T. Chi, R. Cho, S. A. Sheth, W. Goodman, and B. Aazhang, "Emvelop stimulation: minimally invasive deep brain stimulation using temporally interfering electromagnetic waves," *Journal of Neural Engineering*, vol. 19, no. 4, p. 046005, 2022.

[9] B. Hutcheon and Y. Yarom, "Resonance, oscillation and the intrinsic frequency preferences of neurons," *Trends in Neurosciences*, vol. 23, pp. 216–222, 2000.

[10] N. Grossman, D. Bono, N. Dedic, S. B. Kodandaramaiah, A. Rudenko, H.-J. Suk, A. M. Cassara, E. Neufeld, N. Kuster, L.-H. Tsai, A. Pascual-Leone, and E. S. Boyden, "Noninvasive Deep Brain Stimulation via Temporally Interfering Electric Fields," *Cell*, vol. 169, 2017.

[11] S. M. Bawin, L. K. Kaczmarek, and W. R. Adey, "Effects of modulated VHF fields on the central nervous system," *Annals of the New York Academy of Sciences*, vol. 247, pp. 74–81, 1975.

[12] S. M. Bawin, R. J. Gavalas-Medici, and W. R. Adey, "Effects of modulated very high frequency fields on specific brain rhythms in cats," *Brain Research*, vol. 58, pp. 365–384, 1973.

[13] S. M. Bawin and W. R. Adey, "Sensitivity of calcium binding in cerebral tissue to weak environmental electric fields oscillating at low frequency." *Proceedings of the National Academy of Sciences of the United States of America*, vol. 73, 1976.

[14] R. J. MacGregor, "A possible mechanism for the influence of electromagnetic radiation on neuroelectric potentials," *IEEE Transactions on Microwave Theory and Techniques*, vol. 27, no. 11, pp. 914–921, 1979.

[15] F. S. Barnes and C.-L. J. Hu, "Model for some nonthermal effects of radio and microwave fields on biological membranes," *IEEE Transactions on Microwave Theory and Techniques*, vol. 25, no. 9, pp. 742–746, 1977.

[16] A. C. Govindaraju, I. H. Quraishi, A. Lysakowski, R. A. Eatock, and R. M. Raphael, "Nonquantal transmission at the vestibular hair cell–calyx synapse: KLV currents modulate fast electrical and slow K+ potentials," *Proceedings of the National Academy of Sciences*, vol. 120, no. 2, p. e2207466120, 2023.

[17] W. Thomson, "Iii. on the theory of the electric telegraph," *Proceedings of the Royal Society of London*, no. 7, pp. 382–399, 1856.

[18] A. L. Hodgkin and A. F. Huxley, "Currents carried by sodium and potassium ions through the membrane of the giant axon of Loligo," *The Journal of physiology*, vol. 116, no. 4, p. 449, 1952.

[19] COMSOL Multiphysics. [Online]. Available: https://www.comsol.com